

PART I · THE HYDROGEN BOND AND PROTONIC SPECIES

1 The hydrogen bond and chemical parameters favouring proton mobility in solids

ANTOINE POTIER

Proton conduction in solids via hydrogen bonding was suggested in 1950 by Ubbelohde & Rogers¹. Later, the Grotthuss mechanism or translocation² was proposed to explain the conductivity of para-electric potassium dihydrogen phosphate, KDP³, and claimed soon after also for $\text{H}_3\text{O}^+\text{ClO}_4^-$, oxonium perchlorate, OP⁴. Reviews that classified protonic superionic conductors, PSC, appeared from 1980 and were based successively on the ion-exchange properties of materials^{5,7}, their structures^{6,7} and their conduction mechanisms^{8–10}.

In this chapter, the first part (Sections 1.1–1.3) deals with the conduction mechanisms, while the second part (Sections 1.4 and 1.5) points out the significant structural and chemical factors leading to the different conduction mechanisms. The hydrogen bond is a common feature and serves as Ariadne's thread*.

1.1 *From ionic to protonic conduction*

1.1.1 *Ionic conduction*

Ionic conductors may be divided¹¹ into three classes depending on their defect concentrations (i) dilute point defects, dpd ($\sim 10^{18}$ defects cm^{-3}), (ii) concentrated point defects, cpd, ($\sim 10^{18-20}$ cm^{-3}) and (iii) liquid-like or molten salt sublattice materials, mss, ($\sim 10^{22}$ cm^{-3}).

For dilute and concentrated point defect materials, examples are, respectively, NH_4ClO_4 ($\sigma_{250^\circ\text{C}} = 10^{-9} \Omega^{-1} \text{cm}^{-1}$, $E = 1.4$ eV) and CeF_3

* The daughter of Minos and Pasiphae who gave Theseus the thread by which he escaped from the Labyrinth.

The hydrogen bond and protonic species

($\sigma_{240^\circ\text{C}} = 6 \times 10^{-4} \Omega^{-1} \text{cm}^{-1}$, $E = 0.26 \text{ eV}$). The conductivity occurs by an ion hopping mechanism.

In molten salt sublattice materials, practically all the ions in the sublattice are available for motion with an excess of available sites per cation as in e.g. Na β -alumina, ($\sigma_{25^\circ\text{C}} = 1.4 \times 10^{-2} \Omega^{-1} \text{cm}^{-1}$, $E = 0.16 \text{ eV}$). This leads to a high degree of disorder of these cations. The site occupancies and the conductivity characteristics for some of these salts are given in reference 12, pp. 49 and 53. Conduction is favoured by a levelling of the energy profile along the conduction pathway¹³.

Crystalline solid electrolytes have been subdivided¹⁴ into soft ionic crystals such as β - PbF_2 and hard covalent crystals such as β -alumina. The conduction mechanism can be pictured as involving a 'liquid-like' charge carrier array moving in the vibrating potential energy profile set up by the immobile counterions.

1.1.2 From ionic to protonic conduction

Proton conduction might be expected, *a priori*, to occur either by a mechanism of lone proton migration or proton-carried migration (as an entity such as H_3O^+). The occurrence of these processes is now established and, in both cases, the previously proposed subdivisions (dpd, cpd and mss) are relevant.

Thus, lone proton migration (proton translocation or Grotthuss process) occurs in oxonium perchlorate (cpd or perhaps mss) and potassium hydrogen phosphate (mss).

Proton-carried migration occurs in oxonium β -alumina and hydrogen uranyl phosphate, HUP. Both are of the mss type and belong to the specific subclass of 'vehicle mechanisms' in which H_3O^+ is the mobile species.

*1.2 The lone proton migration mechanism (translocation)**1.2.1 The simplest model for translocation and Bjerrum defects*

The translocation mechanism is shown in Fig. 1.1a, b. It results from the coupling of (a) displacement of H^+ along a hydrogen bond and (b) transport of the H^+ ion from this hydrogen bond to the following one. Such a mechanism can occur only in the presence of L defects, as shown in the Bjerrum theory of ice conductivity (reference 15 and

Proton mobility in solids

Chapters 10 and 11). In this theory, the occurrence of doubly occupied sites (Doppelsetzung, D) and/or empty sites (Lehrstehle, L) in a translocation mechanism (Fig. 1.1b) is postulated.

The necessity of having Bjerrum defects present is illustrated for the network of water molecules in Fig. 1.1c. From (i) to (ii), two H^+ transfers occur simultaneously, in a chain sequence under the influence of an applied field V . In (ii) however, this has resulted in the creation of a reverse field, V' which induces the protons to hop back to their original position. Consequently, long-range H^+ conduction cannot occur.

Consider now, in Fig. 1.1c (iii), the effect of allowing the central water molecule in the network to rotate. This creates a pair of L and D defects in adjacent hydrogen bond positions and, on departure of H^+ from the vicinity of this L, D couple, the V' field is destroyed. Conduction can clearly continue, therefore, and the arrival of a new H^+ ion from the left restores the chain element in (iv) to its original position (i).

1.2.1.1 Translocation pathway models

Four types of translocation have been proposed^{8,9}. These are as follows.

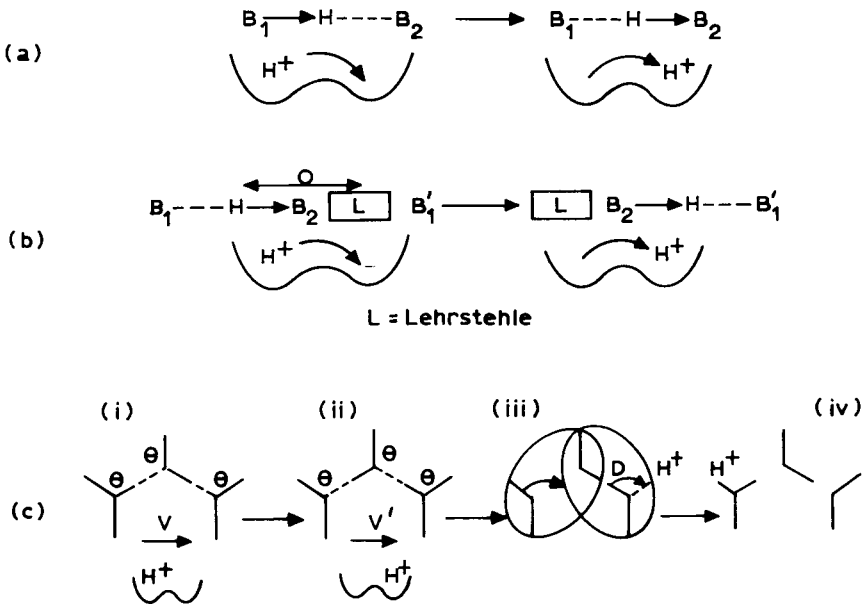


Fig. 1.1.

The hydrogen bond and protonic species

T_1 : anion–cation translocation, e.g. in OP^4 . The T_1 (D/L) mechanism is detailed in Fig. 2 of reference 16.

T_2 : anion chain translocation, e.g. in KDP. The T_2 mechanism for $H_2PO_4^-$ is given in Fig. 1 of reference 3.

T_3 : the translocation of H^+ along a protonated water chain (identical to that for ice); it is detailed in reference 17 for HUP.

T_4 : mixed translocation, for instance in $SnO_2 \cdot 2H_2O$ where⁵ a globular anion $(SnO_{2+x}H_x)^{x-}$ gives a proton to an aqueous chain thereby creating a protonated aqueous chain.

1.2.1.2 From the Bjerrum L, D defects to the molten proton sublattice

Our present state of knowledge does not really confirm or disprove the possible existence of Bjerrum defects, although the potential curve of the proton for L defect propagation in OP has been calculated¹⁶ and appears quite satisfactory. The effect of L and D defects can also be regarded as that occurring from a statistical dynamic disorder of the protons. For example, in crystalline $CsDSO_4$, four H per unit cell are distributed over eight sites in (e) positions and 16 sites in (f) positions¹⁸. This disorder in the H sites and a high site/ H^+ ratio may lead to a quasi-liquid proton sublattice.

1.2.2 A theory for translocation, length of the H bond and crystal field effects

The energy profile for H^+ transport in the translocation model, involving (a) displacement of H^+ along a hydrogen bond, with a transfer energy barrier E_{bar} and (b) transport of H^+ from this hydrogen bond to the next, with a bond breaking energy barrier E_{bond} , is plotted against the oxygen–oxygen distance, d_{o-o} , in Fig. 1.2 for the ion $H_5O_2^+$ in vacuum^{19a, b}. With increasing d_{o-o} , E_{bond} decreases but E_{bar} increases, as in Fig. 1.2b. If we assume that the maximum values for these energy barriers are similar to the activation energy for protonic conduction, E_G , which is usually less than ~ 0.9 eV (or ~ 20 kcal mol⁻¹), then values for d_{o-o} over the range A–B should permit protonic conduction. A refinement of this model in the crystalline state takes account of environmental effects and the energy E_{bond} is replaced by the energy barrier to reorientation of a water molecule, E_{reor} . Since E_{reor} is less than E_{bond} , dashed curve in Fig. 1.2a, the range of permitted values for d_{o-o} is extended to A–C. It can also be seen from Fig. 1.2a that there is an optimum value of d_{o-o} for

Proton mobility in solids

translocation, corresponding to the cross-over of the two curves for E_{bar} and E_{reor} .

Consider now the acid–base couple, $\text{HClO}_4\text{--H}_2\text{O}^{16}$ shown in Fig. 1.3a. In vacuum, it has a potential energy curve with one minimum, corresponding to the isolated Lewis complex $\text{H}_2\text{O} \dots \text{HClO}_4$. On immersing the complex in a Madelung potential, i.e. in a crystal lattice, a double minimum potential curve results. If allowance is then made for polarizability, or an Onsager reaction field, the ionic complex $\text{H}_3\text{O}^+\text{HClO}_4^-$ becomes preferentially stabilized.

The translocation mechanism in this system involves three steps, Fig. 1.3b. These include displacement of H within hydrogen bonds and rotation of the H_3O^+ ions. The effect of the crystal field on the H bond produces the conditions for translocation. This results from the hyperpolarizability of the H bond¹⁹.

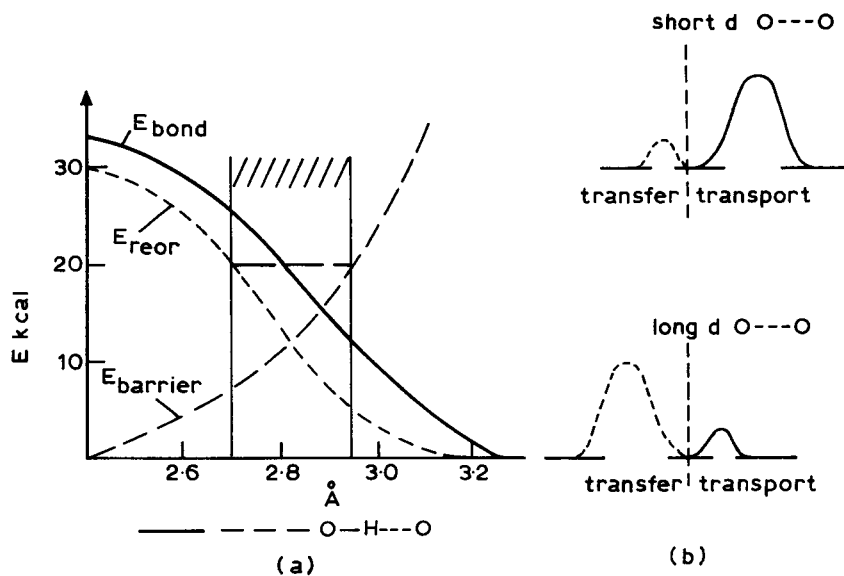


Fig. 1.2.

The hydrogen bond and protonic species

1.3 Proton-carrying mechanisms (the vehicle mechanism or V-mechanism)

1.3.1 Proton-carrying mechanism of the ionic conduction type

As seen previously (Section 1.1.2), the best known example is oxonium β -alumina where the proton carrier is H_2O . In β -alumina, the oxonium ions occupy only BR sites ($E_\sigma = 0.8$ eV; $\sigma_{25^\circ C} = 10^{-11} \Omega^{-1} cm^{-1}$) while in β'' -alumina, oxonium ions can occupy both prismatic and tetrahedral sites ($E_\sigma = 0.6$ eV; $\sigma_{25^\circ C} = 2 \times 10^{-9} \Omega^{-1} cm^{-1}$). Conduction depends on

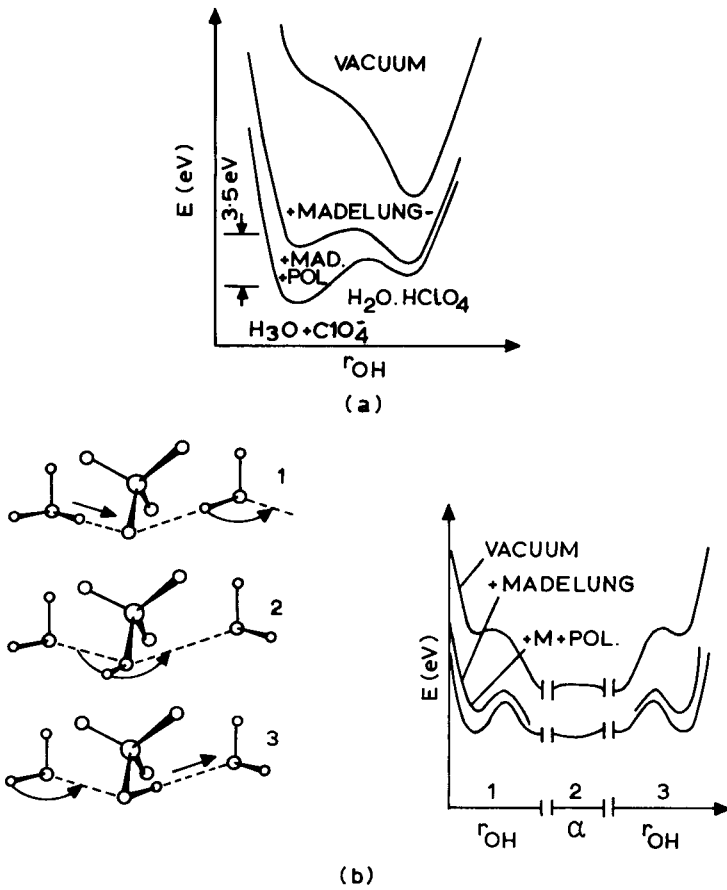


Fig. 1.3.

Proton mobility in solids

an excess of available sites. The mechanism can be close to either a cpd or an mss type.

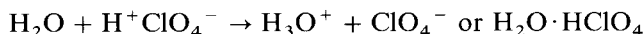
1.3.2 Proton-carrying mechanism for water-rich materials: the vehicle mechanism (V)

In this case, the T_3 translocation (Section 1.2.1.1) is often accepted as the likely mechanism. In 1982, however, a new mechanism called the ‘vehicle mechanism’ was proposed²⁰. At first sight, it resembles the previous proton-carrying process (Fig. 1.3a). It differs, however, in that the proton migrates in one direction as OH_3^+ , NH_4^+ , etc. bonded to a ‘vehicle’ such as H_2O , NH_3 etc. whereas the ‘unladen’ vehicles move in the opposite direction (see, for example, Fig. 1.5b). The explanation given here is that proposed by Rabenau. In this mechanism of cooperative motion, in which the counter-flow of protons and vehicles is essential, voids are created by thermal activation, as in free volume theory.

1.4 Structural effects

Proton-conducting materials have rather special structures^{6,7}, ion-exchange and acid-base properties^{5,7}. It is necessary to take into account the presence of either cation vacancies (such as H_3O^+ vacancies) and voids or H^+ site vacancies.

The structural chemistry in these materials is essentially that of H bonds, that is to say the behaviour of different pairs of bases towards H^+ , for example H_2O and ClO_4^- towards H^+ in



This leads not only to the partial or total internal ionization of the material⁵ but also influences the conduction mechanism.

The crystal structures of proton conductors depend on (a) the anionic part of the material, (b) the cationic part and (c) the defects. Anions can be: (1) monomeric spheres such as ClO_4^- ; (2) polymeric layers as in β -alumina; (3) polymeric channelled skeletons as in antimonic acid hydrates; and (4) drowned oxoanion clusters in water, as in heteropolyacid hydrates.

The cationic part of the material can be: (i) the proton in oxyhydroxyanions, (ii) the oxonium ion in OP; and (iii) the hydrated oxonium

The hydrogen bond and protonic species

ion in HUP. A crystal structure is therefore described by anion–cation combinations such as 1.ii for OP (see Fig. 11.1 p. 166).

Note that most of the proposed combinations are written as ionic formulae. It must be pointed out (Table 1.1), however, that, in acid hydrates, the acidic function is often not entirely ionized. This factor is taken into account as and when necessary.

Finally, the occurrence of different types of defects can serve as a guide in the identification of the H^+ migration mechanism. The defects can be H_3O^+ (or $H_5O_2^+$) defects that occur either as (a) thermally activated (Frenkel) excess sites, such as are present in ionic cpd materials, (b) voids in a quasi-liquid sublattice²⁰, (c) proton defects in the same sense as oxonium defects in a rigid sublattice or (d) proton voids occurring in a quasi-liquid proton sublattice.

1.4.1 Monomeric anions

The oxyhydroxy anion salts, KDP ($\sigma_{25^\circ C} = 10^{-8} \Omega^{-1} \text{cm}^{-1}$; $E_\sigma = 0.55 \text{ eV}$), CsHSO_4 ($\sigma_{150^\circ C} = 10^{-2} \Omega^{-1} \text{cm}^{-1}$; $E_\sigma = 0.33 \text{ eV}$) (see Chapter 11) and $\text{Cs}_3\text{H}(\text{SeO}_4)_2$ ($\sigma_{190^\circ C} = 10^{-3} \Omega^{-1} \text{cm}^{-1}$; $E_\sigma = 0.36 \text{ eV}$) have layered structures. Vacant H^+ defects have been identified¹⁸. The more numerous the defects, the flatter the potential along the conduction pathway. KDP is of the (c) type (T_2 mechanism) while the others are of the (d) type (quasi-liquid H^+ sublattice).

In the orthorhombic phase of OP ($\sigma_{25^\circ C} = 3.5 \times 10^{-4} \Omega^{-1} \text{cm}^{-1}$; $E_\sigma = 0.36 \text{ eV}$), rows of H_3O^+ ions are oriented along the three crystallographic axes. Excess oxonium sites occur only by thermal activation and the contribution of ionic cpd to conductivity is probably weak⁴. On the other hand, an excess of available proton sites^{21,22} lowers considerably the barrier to H_3O^+ rotation. The reorientation energy, E_{reor} (see Fig. 1.2a), is much less than the activation energy for conduction, E_σ , which is essentially given by the energy barrier, E_{bar} to displacement within the hydrogen bond¹⁶. This is consistent with long bonds, $d_{\text{o-o}}$, in OP: $2.92 < d_{\text{o-o}} < 2.99 \text{ \AA}$.

HUP²³ (see p. 261) and $\text{UO}_2(\text{H}_2\text{PO}_4)_2 \cdot 3\text{H}_2\text{O}^{24}$ have layered structures with H-bonded PO_4^{3-} ions. The analysis¹⁸ of H^+ defects in HUP leads to a low energy along the pathway so that a (T_3) conduction mechanism is possible. On the other hand, measurement of ^{18}O and H diffusivities have demonstrated a vehicle, V, mechanism by oxonium ions²⁵.

*Proton mobility in solids**1.4.2 Layered polymeric anions (see Chapters 13 and 23)*

The best example is H_3O^+ β -alumina ($\sigma_{25^\circ\text{C}} = 10^{-10} \Omega^{-1} \text{cm}^{-1}$; $E_\sigma = 0.6 \text{ eV}$); it is a relatively poorly conducting material with H_3O^+ ions hopping into vacant sites; conduction is not a V process. This material is completely ionized owing to the poor basicity of the layers (Section 1.5.1.1). In the case of $(\text{NH}_4^+)(\text{H}_3\text{O}^+)$ β'' -alumina single crystal²⁶, ($\sigma_{25^\circ\text{C}} = 10^{-3} \Omega^{-1} \text{cm}^{-1}$; $E_\sigma = 0.3 \text{ eV}$), the data do not lead to an unambiguous choice between T_3 and V mechanisms, nor do H diffusion pulse field gradient, PFG or NMR measurements²⁷.

The best example of an oxonium hydrate salt is $\text{H}_3\text{O}^+(\text{H}_2\text{O})_n$ β'' -alumina ($\sigma_{25^\circ\text{C}} = 6.5 \times 10^{-6} \Omega^{-1} \text{cm}^{-1}$; $E_\sigma = 0.15 \text{ eV}$). The low value of the activation energy is an argument for a V process and the low conductivity might be due to the small number of available sites for such a process, owing to saturation of the crystal. However, serious arguments for a T_3 translocation mechanism have been given^{28,29}.

1.4.3 Channelled polymeric anions

Polyantimonic acid hydrates can be written either as $\text{Sb}_2\text{O}_5 \cdot m\text{H}_2\text{O}$ or $\text{HSbO}_3 \cdot n\text{H}_2\text{O}$. Crystals with $n = 1, 1/2, 1/3, 1/4$ are known to possess interconnected channels. The activation energies are near 0.4 eV while $\sigma_{25^\circ\text{C}}$ decreases with n for all except the cubic $n = 1$, Fd3 phase. All reported studies indicate that conductivity occurs by translocation. For $n = 1$ the channel is populated by a continuous H bond network (Section 1.5.1.2) which is sometimes disrupted. The mechanism seems to result from the small diameter of the channels.

Ammoniated zeolites present the counter example (see Chapter 14). Large cavities are connected by short channels, the bottleneck effect of which governs the conductivity laws³⁰. The $\log \sigma/(1/T)$ curves are representative of a V process (Fig. 1 in reference 30). They do not obey an Arrhenius law.

1.4.4 Drowned oxoanion clusters

Dioxide dihydrates and heteropolyacid hydrates, HPA³¹ (see Chapter 18), are representative examples. Following reference 5, in $\text{SnO}_2 \cdot 2\text{H}_2\text{O}$ ($\sigma_{25^\circ\text{C}} = 10^{-4} \Omega^{-1} \text{cm}^{-1}$; $E_\sigma = 0.2 \text{ eV}$), 25 Å anion-clusters are surrounded by a bed of water forming a quasi-liquid phase (intercluster gap ~ 6 Å). SnO_2 is partly hydroxylated (Section 1.5.1.1). A V process can be

The hydrogen bond and protonic species

inferred from the proposed E_{σ} value⁵ jointly with a cluster–water translocation that cannot be disregarded *a priori*.

HPA hydrates^{31–33}, $n = 6, 14, 21, 29$, give 12 Å clusters such as $[\text{PW}_{12}\text{O}_{40}]^{3-}$. They are very good PSC with e.g. for $n = 21$, $\sigma_{25^{\circ}\text{C}} = 0.15 \Omega^{-1} \text{cm}^{-1}$ and $E_{\sigma} = 0.15 \text{ eV}$. A vehicle mechanism has been proposed from these data^{34,35}. In $\text{HPA} \cdot 21\text{H}_2\text{O}$, however, most of the water-cluster anion H bonds are long while the intrawater bonds are of medium length so that, with practically independent anions, the possibility of a T_3 process cannot be completely disregarded³².

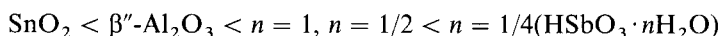
It can be concluded that the H^+ q.l. sublattice really exists as well as the oxonium q.l. sublattice. The experimental distinction between them remains subtle; even PFG measurements can have different interpretations and only the challenge of experimental facts³⁴ can shed some new light.

1.5 Chemical ‘equilibrium’ and the ‘ionic defect’: towards a chemical classification**1.5.1 The acidity–basicity effect, the ‘ionic defect’ and the H bond hyperpolarizability****1.5.1.1 Acidity in solid materials, surface acidity, condensation**

Acidity–basicity effects must always be taken into account to explain the properties of oxygenated material. Thus, in strong acids, proton transfer to water is complete but this is not so for weaker acids and amphoteric materials.

Acidity–basicity effects in proton-conducting materials depend not only on the atomic and bonding properties of the central anionic species, but also on the properties of the aggregate surface and on the state of aggregation as can be observed in a discussion of the true compositions of weak and medium strength acidic materials such as tin dioxide, β'' -alumina and antimononic acid hydrates (Table 1.1).

Taking as a measure of acidity the true oxonium concentration (mole fraction) in the cationic sublattice, the order of increasing acidity seems to be



The behaviour of antimononic acid depends on the water/ Sb_2O_5 ratio in $\text{Sb}_2\text{O}_5 \cdot m\text{H}_2\text{O}$ compounds. That of SnO_2 and β'' -alumina is more difficult